Fundamentally different global marine nitrogen cycling in response to extreme ocean deoxygenation

B. David A. Naafs[1,*,+], Fanny M. Monteiro[2*], Ann Pearson[3], Meytal B. Higgins[4], Rich D. Pancost[1], and Andy Ridgwell[2,5]

[1]Organic Geochemistry Unit, School of Chemistry, School of Earth Sciences, the Cabot Institute for the Environment, University of Bristol, Bristol, UK

[2]School of Geographical Sciences, University of Bristol, Bristol, UK

[3]Department of Earth and Planetary Sciences, Harvard University, Cambridge, USA

[4]ExxonMobil Research & Engineering, Annandale, USA

[5]Department of Earth and Planetary Sciences, University of California-Riverside, Riverside, CA, USA

[*]These authors contributed equally

[+]Corresponding author david.naafs@bristol.ac.uk (David Naafs)

Abstract

The present-day marine nitrogen (N) cycle is strongly regulated. Deficiencies in the availability of fixed and readily bioavailable nitrogen (N_{fixed}) relative to phosphate (P) in the surface ocean are largely corrected by the activity of N fixers. This feedback system, termed the "nitrostat", is thought to have provided close regulation of N_{fixed} speciation and inventory relative to P since the Proterozoic. In contrast, during intervals of intense deoxygenation such as Cretaceous Ocean Anoxic Event (OAE) 2, a few regional sedimentary $\delta^{15}N$ records hint at the existence of a different mode of marine N-cycling in which ammonium plays a major role in regulating export production. However, the global-scale dynamics during this time remain unknown. Here, using an Earth System model and taking the example of OAE 2, we provide new insights into the global marine nitrogen cycle under severe ocean deoxygenation. Specifically, we find that the ocean can exhibit fundamental transitions in the species of nitrogen dominating the N_{fixed} inventory – from NO_3^- to NH_4^+ – and that as this transition occurs, the N_{fixed} inventory can partially collapse relative to P due to progressive spatial decoupling between the loci of NH_4^+ oxidation, NO_3^- reduction, and fixation of nitrogen. This finding is relatively independent of the specific state of ocean circulation and is consistent with nitrogen isotope and redox proxy data. The substantive reduction in the ocean N_{fixed} inventory at an intermediate state of deoxygenation may represent a biogeochemical vulnerability with potential implications for past and future (warmer) oceans.

Significance statement

The ratio of the dissolved inventories of readily bio-available (fixed) nitrogen (N) to phosphorous (P) is regulated close to 16:1 in the modern, well-oxygenated ocean. This situation – fixed nitrogen tracking P – is generally assumed to have operated for hundreds of millions of years. Here we use computer simulations combined with proxy data to instead demonstrate that the marine nitrogen cycle operates very

45 differently when dissolved oxygen concentrations in the ocean are lower than
46 present. Not only is nitrate replaced by ammonium as the dominant component of
47 fixed nitrogen, but the total fixed inventory collapses relative to P. This makes the
48 strength and state of the biological pump in the ocean highly susceptible to
49 disruption, with potential past and future implications.
50 /body

Introduction

Nitrogen (N) is an essential nutrient for life, and in the modern ocean, small regional differences in the bioavailability of N induce large differences in primary productivity, ecosystem dynamics, and biogeochemical cycles (1-3). The ocean inventory of the readily bioavailable or 'fixed' forms of N, primarily nitrate (NO_3^-) and ammonium (NH_4^+), is ultimately governed by the balance between denitrification predominantly in oxygen minimum zones (OMZs) and N fixation by diazotrophs mainly in the (sub)tropical gyres (4-6). Importantly, these processes are connected on a global scale, as an increased loss of fixed N relative to phosphorus (P) favors organisms that perform the energetically costly process of N fixation. As such, the marine N cycle shapes modern nutrient and ecosystem dynamics and in this system of negative feedbacks, the N:P ratio and hence fixed N inventory of the ocean are tightly regulated. Known as the "nitrostat", these feedbacks are assumed to have been relatively stable since the proliferation of N fixers in the (late) Proterozoic (5).

This assumption that strong negative feedbacks stabilize the oceanic N inventory, speciation, and productivity tends to frame our interpretation of future scenarios (7) and past events (8), including Oceanic Anoxic Events (OAEs). The OAEs occurred predominantly during the Mesozoic and are associated with widespread ocean deoxygenation and perturbations of major biogeochemical cycles, including the marine N cycle (9). For example, OAEs are associated with depleted bulk sediment nitrogen isotope ($\delta^{15}N_{bulk}$) values in some parts of the (proto-) Atlantic ocean (10, 11). The classical hypothesis for the operation of the marine N cycle in an extremely deoxygenated ocean – such as occurred during the OAEs – argues that primary production was dominated by N_2-fixing cyanobacteria (11, 12) to counter the high rates of N-loss in the expanded OMZs, resulting in low $\delta^{15}N_{bulk}$ values. This would be generally consistent with our understanding of a dominance of nitrostat-driven negative feedbacks between denitrification and N fixation in the modern oceans, stabilizing the oceanic inventory of fixed N (1, 2, 4).

However, the very negative (< -2 ‰) $\delta^{15}N_{bulk}$ and even more depleted (< -4 ‰) chlorophyll-derived porphyrin N isotopes ($\delta^{15}N_{por}$) from the (equatorial) Atlantic across OAE 2 suggest a contribution, potentially major, from eukaryotic primary producers assimilating recycled ammonium (10, 13, 14). This hints at a very different operation of the marine N cycle under conditions of extreme ocean deoxygenation, in which ammonium availability may be high enough to play a major role in regulating export production, at least in the equatorial Atlantic. Similarly, very depleted $\delta^{15}N_{bulk}$ (minima ~ -3 ‰) have been found in semi-restricted shelf basins of the Tethys Ocean during the Paleocene Eocene Thermal Maximum (PETM) (15), suggesting an important role for ammonium assimilation during this transient global warming event. Together, these observations suggest that ammonium assimilation might be inherent to deoxygenation events during the Phanerozoic and may reflect the changing balance in redox speciation of the major components of dissolved inorganic nitrogen (DIN), namely: NO_3^- and NH_4^+ (together: the fixed nitrogen pool).

However, these observations highlight a major challenge: resolving the role and strength of marine N cycle feedbacks is complicated by the fact that evidence recorded in the sediments is fragmented and reflects local, not global processes (16). For OAE 2, virtually all proxy data are from the (central) Atlantic and Tethys Ocean (10). In addition, the proxy record predominantly reflects surface ocean processes, limiting our understanding of N cycle dynamics in the ocean's interior and hence the dominant reservoir of N in the intermediate and deep ocean; upwelling of this deep reservoir supports much of primary production in modern systems, and presumably in ancient ones as well. Furthermore, although models have been used to study the marine N cycle during OAE 2 (10, 14), these models have tended to either focus on a regional scale, and the area of the (proto-) Atlantic and Tethys Ocean (11), or only on the average surface vs. average deep ocean (14). Assessment of the marine N cycle dynamics in a fully 3-dimensional and global context, as well as a more generalized understanding of how global N cycling responds to extreme ocean deoxygenation

events, is still needed. To elucidate global-scale marine N cycle dynamics as the ocean is progressively deoxygenated, here we used an Earth System model of intermediate complexity ('GENIE') (17) and as a case study used Cenomanian-Turonian OAE 2 (~93 Ma), one of the most extreme ocean deoxygenation events of the last 250 Ma.

Results

In our simulations, as the oceanic phosphorus inventory increases, the associated increase in export production causes the oxygen content of the ocean to decrease, leading to expanded anoxia, here defined as 0 µmol/l O_2 (Fig. 1a). All simulations with more than 1 x PO_4^{3-} have enhanced export production and an expanded extent of photic zone euxinia (PZE) compared to modern, in agreement with previous box model studies (18, 19). In the highest (4 x PO_4^{3-}) scenario, export production is more than four times higher than modern rates, and the upper depth boundaries of the OMZs impinge on the photic zone, leading to PZE in ~35% of the ocean (Fig. 1a). Within the euxinic OMZs, organic matter remineralization is predominantly mediated by sulfate reduction, contributing to 21% of total OM remineralization globally (SI Appendix, Fig. S3).

Our phosphate inventory-induced changes in the extent of ocean oxygenation have a profound impact on the marine N cycle, and in particular, on which species of N dominates the fixed nitrogen pool: nitrate or ammonium. In our model, an increase from 0.25 to 1 x PO_4^{3-} concentration enhances primary production ~4-fold, from 2.2 to 8.6 Gt C yr^{-1}, and leads to an increase in the fixed N inventory (NO_3^- + NH_4^+) of the ocean by around 200% due to a compensating increase in N_2 fixation (Fig. 1b-d). Notably, this is far short of the 400% increase that would have been necessary to maintain a mean N:P ocean inventory of 16:1, the reasons for which we discuss later. The marine N cycle in the 1 x PO_4^{3-} simulation (4 x CO_2, and Cenomanian paleogeography) differs from the results for the modern (Table 1). In our

Cenomanian simulations, the fixed N inventory does not reach modern values until the 4 x PO_4^{3-} simulations (Fig. 1b), highlighting the role of atmospheric CO_2 and paleogeography (affecting temperature and ocean currents, respectively) in modulating the state of marine N cycling, in addition to changes in the oceanic phosphate inventory. In the Cenomanian simulation, higher temperatures and different ocean circulation deplete the N inventory compared to modern (Fig. 1c), implying that future warmer, deoxygenated conditions could also reduce the global ocean N inventory.

As phosphate concentrations increase towards 4 x PO_4^{3-}, the fraction of the ocean that is anoxic expands, and denitrification rates increase, resulting in up to ~15% of global organic matter being remineralized via NO_3^- respiration. The value of ~15% appears to be an inherent limit for the global contribution of denitrification to organic remineralization (SI Appendix, Fig. S3). This, in turn, places a limit on the loss of "fixed" N and ultimately leads to a maximum contribution of N fixation to export production of ~55-60% for an ocean with widespread anoxia but operating under an oxygen-rich atmosphere (Fig. 1d). This limit is due to geographic restriction of denitrification, which mainly occurs at the edge of the OMZs, where oxygen is low enough for denitrification, yet nitrification rates remain high enough to produce nitrate. As oxygen content in the ocean decreases, higher rates of denitrification, combined with lower nitrification rates, result in a sharp decline in nitrate concentration, reducing the eventual contribution of upwelled nitrate to export production (Fig. 1b-d).

Because nitrification of NH_4^+ requires oxygen, NH_4^+ accumulates in the ocean, mostly in the OMZs. In the 4 x PO_4^{3-} ocean, average NH_4^+ concentrations reach up to two orders of magnitude higher than in the modern ocean (Fig. 1b), reaching values similar to those only observed in the modern in the OMZ of the Black Sea (20). In such an "ammonium ocean", NH_4^+ assimilation does not dominate the source of nutrient nitrogen for export production globally, constituting at most 22% of

163 total export production (Fig. 1d). This is because most of the upwelled NH_4^+ is
164 nitrified in oxygenated layers underlying the photic zone. However, where local NH_4^+
165 assimilation occurs, it can contribute > 30% of export production, for example in the
166 tropical proto-Atlantic. The relative contribution of N_2 fixation and NH_4^+ assimilation to
167 export production is thus controlled by the spatial structure of the OMZ relative to the
168 base of the photic zone, which in turn is controlled by ocean circulation (i.e.,
169 upwelling regions). When the OMZ impinges the photic zone, NH_4^+ becomes
170 available for direct assimilation by phytoplankton. When the OMZ is spatially
171 separated from the photic zone, nitrification (and subsequent denitrification) reduce
172 the availability of NH_4^+ to the photic zone.
173 However, our results collectively demonstrate that the system does not
174 monotonically transition from a “nitrate” to an “ammonium” ocean as oxygen
175 progressively declines. Under intermediate conditions in the transition (in our
176 Cenomanian simulations: 2 x PO_4^{3-}), a unique state of N cycling occurs in which the
177 ocean is not yet anoxic enough to develop extensive OMZs rich in ammonium.
178 Relatively high rates of nitrification restrict the accumulation of NH_4^+, yet at the same
179 time, high rates of denitrification keep the ocean nitrate inventory low (Fig. 1d). As a
180 result, the ocean becomes extremely depleted in all forms of fixed N (Fig. 1c).
181
182 **Discussion**
183 Contrary to earlier studies (21, 22), our results show how the deep ocean can
184 become highly depleted in “fixed” N (Fig. 2b) relative to phosphate, leading to a
185 biogeochemical state that contrasts markedly to the modern oxic ocean. As
186 phosphate concentrations increase and anoxia expands, the ocean transitions from a
187 feedback-balanced system where the nitrate inventory tracks phosphate (23), to a
188 state in which the deep ocean becomes highly depleted in nitrogen relative to
189 phosphorus (Fig. 1c). And rather than a NO_3^--replete deep ocean (Fig. 3a), the
190 dominant form of nitrogen becomes NH_4^+, which is furthermore localized to expanded

191 OMZs and does not “fill” all of the deep ocean (Table 1 and Fig. 3b-c). This
192 transformation occurs in the model despite high rates of N fixation at the surface and
193 concomitantly high export production fluxes of particulate organic nitrogen into the
194 ocean interior – both factors that should favor a large deep ocean N_{fixed} inventory of
195 NH_4^+ released from organic matter remineralization.

196 But did this ocean state really develop? Proxy data for bottom water anoxia
197 and photic zone euxinia during OAE 2 best match the 2 x PO_4^{3-} simulation (24).
198 Although there are a number of uncertainties and caveats associated with both the
199 model simulations and proxy data, the 2 x PO_4^{3-} scenario also is the same ocean
200 phosphate scenario that yields a marine N cycle simulation with minimum total N_{fixed}
201 inventory (Fig. 1c). In this simulation, 11% of the total volume of the ocean (Fig. 1a)
202 and 16% of the sea floor is anoxic (defined here as 0 µmol/l O_2) (Table 1), consistent
203 with uranium isotope data that indicate that 8-15% of the sea floor became anoxic
204 during OAE 2 (25). We argue that the existence of an elevated oceanic phosphate
205 inventory compared to the modern is consistent with calcium isotope measurements
206 that indicate an increased weathering flux (26) and hence presumably, increased rate
207 of PO_4^{3-} supply to the ocean. Together with the likelihood that phosphorous was more
208 strongly regenerated from the ocean floor under anoxic conditions (27), an increased
209 PO_4^{3-} state is a reasonable outcome, and the relatively conservative 2 x PO_4^{3-}
210 amplification (rather than 3 x or 4 x PO_4^{3-}) is the scenario that leads to the greatest
211 reduction in N_{fixed} inventory.

212 In the 2 x PO_4^{3-} simulations, N fixation is the most intense in equatorial
213 upwelling regions and in the Pacific sector of the Southern Ocean, where deep and
214 denitrified waters with low N:P ratios reach the photic zone (Fig. 2). Globally, NH_4^+-
215 assimilation is significant but is not the dominant source of nutrient nitrogen for
216 marine production, contributing ~10% of total export production (Table 1). Regionally,
217 however, NH_4^+-assimilation is important in the most intensely anoxic and/or upwelling
218 regions, such as the euxinic equatorial Atlantic (Fig. 2).

Available nitrogen stable isotope data for OAE 2 allow for comparison with our model simulations, although published data to date are restricted to the (proto)-Atlantic and Tethys Ocean. Firstly, records from the equatorial Atlantic (Demerara Rise sites and Site 367) show extremely depleted $\delta^{15}N_{bulk}$ values during OAE 2, with minima of < -3‰ and average values around -2‰ (12-14). These depleted $\delta^{15}N$ values are interpreted to reflect a region dominated by N fixation and/or NH_4^+ assimilation, although it is difficult to detangle the individual importance of each process (14). Our model simulations are in concordance, with a relatively large contribution of N_2 fixation and especially NH_4^+ assimilation (> 30 %), to export production in this region (Fig. 2a). By contrast, the continental margins of Europe and North America are characterized by enriched ($\delta^{15}N_{bulk}$ values around 1‰), even during the peak of OAE 2 (10). This is also consistent with our simulations, which indicate a low contribution of N fixation and NH_4^+ assimilation to export production on those particular margins, with productivity instead dominated by NO_3^-. Sites in the subtropical Atlantic (Sites 386, 1276, and 641) (10) are characterized by negative $\delta^{15}N_{bulk}$ values (average values around -1‰), although less negative then those recorded in the equatorial Atlantic (averages around -2‰). Our simulations are largely consistent with these intermediate $\delta^{15}N_{bulk}$ values, as the surface ocean at Sites 368 and 641 is characterized by a high contribution of N fixation to export production (> 70 %), but no major influence of ammonium assimilation. Site 1276 is an exception to the general agreement between our model simulations and published interpretations of $\delta^{15}N_{bulk}$ proxy data. In our simulations, this location is not characterized by high contributions of N fixation and/or NH_4^+ assimilation that would lead to depleted $\delta^{15}N_{bulk}$, yet the available $\delta^{15}N_{bulk}$ values are negative. Overall our simulations compare well with the proxy record from the Atlantic and Tethys Ocean as well as regional box modelling studies (10, 13, 14, 28), providing additional confidence.

Both the proxy record and box modelling studies to date are limited to the Atlantic and Tethys Ocean. Our simulations also suggest that NH_4^+-assimilation may have fueled export production in parts of the eastern equatorial Pacific, and that N-fixation was important across the equatorial Pacific and Indian Ocean and in the high-latitude southern Pacific Ocean. However, formal assessment of these model predictions will have to await new data from these basins.

If the marine N cycle of OAE 2 can maintain a fundamentally different structure from the modern version, one might expect comparably different N cycle states to occur at other times in Earth history. For example, late Devonian black shales (29) as well as Paleocene Eocene Thermal Maximum (PETM) black shales (15) are characterized by depleted $\delta^{15}N_{bulk}$ values similar to those reported for OAE 2. The climate state and paleogeography, which determine the specific sensitivity of the marine N cycle to changes in oxygenation state, were different during those events compared to OAE 2. However, the same mechanisms and feedback processes identified for the OAE 2 scenario presumably would operate. If the anoxia was intense enough, these events also may have promoted a depletion in bio-available N; and incorporation of ammonium may have been important in euxinic (semi)-restricted basins (e.g., the Northeast Tethys during the PETM). A low- N_{fixed} inventory in the deep Proterozoic ocean has also been proposed (21, 30), but arises because of low productivity (low PO_4^{3-}) and low atmospheric oxygen concentrations (pO_2); that scenario is in stark contrast to the Phanerozoic scenarios modeled here, in which ocean PO_4^{3-} concentrations and productivity are *higher* than modern.

Changing the global N inventories and spatial patterns of N cycling also has far-reaching implications for marine ecology and attendant proxies, and other biogeochemical cycles. For example, the habitat for ammonia-oxidizers (e.g., Thaumarchaeota) may have been very different in a reorganized, low-oxygen N cycle. These organisms may have moved to shallower depths if they were able to resist photoinhibition and other associated oxidative pressures. This shift in habitat

may then influence TEX_{86}-based temperature estimates in anoxic basins, as existing calibrations are based on modern systems in which the organisms primarily reside below the base of the photic zone. Marine N_2O production likely would also have increased during anoxic events due to elevated rates of both denitrification and nitrification (31), which characterize some of the main pathways of N_2O production in the ocean (32). If the N_2O cycle shifted closer to surface waters, thereby increasing gas evasion rates, N_2O could have provided a powerful positive feedback mechanism to sustain the OAE. N_2O is a potent greenhouse gas, 1000 times more effective than CO_2, and its release could partially offset the negative feedback on warming of the expansion in organic carbon burial. The interplay of such processes could account for the rather complex temperature changes observed across OAE 2 (33).

The scenarios modeled here may also have important implications for future climate change. Over the past 50 years the oxygen content of the ocean has declined (34) and is expected to accelerate with future ocean warming (35). Some regions of the ocean are already close to transitioning to full anoxia (36). Our results illuminate the sensitivity of the marine N cycle to changes in ocean oxygen content, implying that the future ocean may be more vulnerable to N loss than previously recognized, which will have far-reaching consequences for other biogeochemical processes and marine ecosystems.

Conclusions

Our understanding of the response of the marine N cycle to changes in ocean oxygenation largely comes from past perturbation events such as the Ocean Anoxic Events of the Mesozoic, with relatively sparse proxy records and regional models informing most of our understanding to date. Here, we applied a global 3D Earth system model (GENIE), upgraded with a more complete set of N cycle processes, to provide specific insights into the global marine N-cycle associated with OAE 2 as well as to provide generalized understanding of how the marine N cycle responds under

progressively extreme deoxygenation. We find that as phosphate concentrations increase and anoxia expands, the ocean transitions from an oxic state with high concentrations of nitrate to an anoxic/reducing state in which the deep ocean becomes highly depleted in nitrogen relative to phosphorus, with “fixed” nitrogen predominantly in the form of ammonium and mostly geographically restricted to expanded OMZs. These results point to potential breakdown in the feedbacks that were thought to keep global N marine inventories in balance, i.e., the “nitrostat”.

Materials and Methods

All simulations were run using the GENIE model. The code for the version of the GENIE model used in this paper (technically: cGENIE) can be found here: https://svn.ggy.bris.ac.uk/subversion/genie/tags/cgenie-NaafsMonteiro.PNAS.2019 (svn revision 10275) and includes all configuration and boundary condition files (check genie-userconfigs/MS/PNAS2019.NaafsMonteiro for the specific userconfig files). The code on the SVN repository can be accessed with the username: *genie-user* and password: *g3n1e-user*. Documentation on running the cGENIE model can be found in the genie-docs directory of the code installation. As employed here, GENIE includes representations of the marine cycles of phosphorus, nitrogen, oxygen, and sulfur. To extend the applicability of GENIE to a poorly oxygenated ocean, we further developed the N cycle to include second-order substrate limitation of nitrification rates by both ammonium and oxygen rather than just ammonium (see SI Appendix).

We used the already published OAE 2 data-constrained Cenomanian paleogeography configuration of the GENIE model (24), with simulations conducted at 4x pre-industrial atmospheric CO_2 concentrations, and a range of different oceanic phosphate inventories (0.25 to 4 times modern PO_4^{3-}). Although we could have explored the effects of other biogeochemical variables such as imposing changes on atmospheric pO_2 and hence ocean dissolved oxygen concentrations directly, OAEs are widely regarded as being characterized by high levels of pCO_2 (37) and are inferred to be characterized by a higher-than-modern oceanic phosphate. This increased P inventory resulted from extensive submarine volcanism (37, 38) and hence increased terrestrial rock (and apatite mineral) weathering rates (39), in combination with a decreased ocean sink as a consequence of benthic P regeneration under sedimentary anoxia (27). All model scenarios were run for 20 kyr to steady state.

Acknowledgments

We thank Sarah Greene for providing the paleolocations of the sites used in this study. B.D.A.N. is funded through a Royal Society Tata University Research Fellowship. F.M.M. is supported by a NERC research fellowship (NE/J019062/1) and a NERC standard grant (NE/N011112/1). A.P. acknowledges support from the Gordon and Betty Moore Foundation, the NASA Astrobiology Institute, and a Benjamin Meaker Visiting Professorship, University of Bristol. R.D.P. acknowledges the Royal Society Wolfson Research Merit Award. This material is based on work supported by the National Science Foundation under Grant Number 1736771 (to A.R.). A.R. also acknowledges funding from the European Research Council as part of the "PALEOGENiE" project (ERC-2013-CoG-617313).

References

1. Voss M*, et al.* (2013) The marine nitrogen cycle: recent discoveries, uncertainties and the potential relevance of climate change. *Phil. Trans. R. Soc. B* 368(20130121).
2. Moore CM*, et al.* (2013) Processes and patterns of oceanic nutrient limitation. *Nature Geoscience* 6(9):701-710.
3. Falkowski PG, Barber RT, & Smetacek V (1998) Biogeochemical Controls and Feedbacks on Ocean Primary Production. *Science* 281(5374):200.
4. Redfield AC (1958) The biological control of chemical factors in the environment. *American Scientist* 46(3):230A-221.
5. Tyrrell T (1999) The relative influences of nitrogen and phosphorus on oceanic primary production. *Nature* 400(6744):525-531.
6. Deutsch C, Sarmiento JL, Sigman DM, Gruber N, & Dunne JP (2007) Spatial coupling of nitrogen inputs and losses in the ocean. *Nature* 445(7124):163-167.
7. Gruber N & Galloway JN (2008) An Earth-system perspective of the global nitrogen cycle. *Nature* 451:293.
8. Boyle RA*, et al.* (2013) Nitrogen cycle feedbacks as a control on euxinia in the mid-Proterozoic ocean. *Nature Communications* 4:1533.
9. Jenkyns HC (2010) Geochemistry of oceanic anoxic events. *Geochemistry Geophysics Geosystems* 11(3):Q03004.
10. Ruvalcaba Baroni I, van Helmond NAGM, Tsandev I, Middelburg JJ, & Slomp CP (2015) The nitrogen isotope composition of sediments from the proto-North Atlantic during Oceanic Anoxic Event 2. *Paleoceanography* 30(7):923-937.
11. Rau GH, Arthur MA, & Dean WE (1987) $^{15}N/^{14}N$ variations in Cretaceous Atlantic sedimentary sequences: implication for past changes in marine

nitrogen biogeochemistry. *Earth and Planetary Science Letters* 82(3–4):269-279.
12. Kuypers MMM, van Breugel Y, Schouten S, Erba E, & Sinninghe Damsté JS (2004) N_2-fixing cyanobacteria supplied nutrient N for Cretaceous oceanic anoxic events. *Geology* 32(10):853-856.
13. Junium CK & Arthur MA (2007) Nitrogen cycling during the Cretaceous, Cenomanian-Turonian Oceanic Anoxic Event II. *Geochemistry, Geophysics, Geosystems* 8(3):Q03002.
14. Higgins MB, Robinson RS, Husson JM, Carter SJ, & Pearson A (2012) Dominant eukaryotic export production during ocean anoxic events reflects the importance of recycled NH_4^+. *Proceedings of the National Academy of Sciences of the United States of America* 109(7):2269-2274.
15. Junium CK, Dickson AJ, & Uveges BT (2018) Perturbation to the nitrogen cycle during rapid Early Eocene global warming. *Nature Communications* 9(1):3186.
16. Trabucho-Alexandre J*, et al.* (2010) The mid-Cretaceous North Atlantic nutrient trap: Black shales and OAEs. *Paleoceanography* 25(4):PA4201.
17. Ridgwell A*, et al.* (2007) Marine geochemical data assimilation in an efficient Earth System Model of global biogeochemical cycling. *Biogeosciences* 4(1):87-104.
18. Tsandev I & Slomp CP (2009) Modeling phosphorus cycling and carbon burial during Cretaceous Oceanic Anoxic Events. *Earth and Planetary Science Letters* 286(1):71-79.
19. Flögel S*, et al.* (2011) Simulating the biogeochemical effects of volcanic CO_2 degassing on the oxygen-state of the deep ocean during the Cenomanian/Turonian Anoxic Event (OAE 2). *Earth and Planetary Science Letters* 305(3-4):371-384.
20. Konovalov SK, Ivanov LI, & Samodurov AS (2000) Oxygen, nitrogen and sulphide fluxes in the Black Sea. *Mediter. Mar. Sci.* 1(2):41-59.
21. Fennel K, Follows M, & Falkowski PG (2005) The co-evolution of the nitrogen, carbon and oxygen cycles in the Proterozoic ocean. *American Journal of Science* 305(6-8):526-545.
22. Saltzman MR (2005) Phosphorus, nitrogen, and the redox evolution of the Paleozoic oceans. *Geology* 33(7):573-576.
23. Lenton TM & Watson AJ (2000) Redfield revisited: 1. Regulation of nitrate, phosphate, and oxygen in the ocean. *Global Biogeochemical Cycles* 14(1):225-248.
24. Monteiro FM, Pancost RD, Ridgwell A, & Donnadieu Y (2012) Nutrients as the dominant control on the spread of anoxia and euxinia across the Cenomanian-Turonian oceanic anoxic event (OAE2): Model-data comparison. *Paleoceanography* 27(4):PA4209.
25. Clarkson MO*, et al.* (2018) Uranium isotope evidence for two episodes of deoxygenation during Oceanic Anoxic Event 2. *Proceedings of the National Academy of Sciences* 115(12):2918-2923.
26. Blättler CL, Jenkyns HC, Reynard LM, & Henderson GM (2011) Significant increases in global weathering during Oceanic Anoxic Events 1a and 2 indicated by calcium isotopes. *Earth and Planetary Science Letters* 309(1-2):77-88.
27. Van Cappellen P & Ingall ED (1994) Benthic phosphorus regeneration, net primary production, and ocean anoxia: A model of the coupled marine

biogeochemical cycles of carbon and phosphorus. *Paleoceanography* 9(5):677-692.
28. Ruvalcaba Baroni I, Tsandev I, & Slomp CP (2014) Enhanced N_2-fixation and NH^{4+} recycling during oceanic anoxic event 2 in the proto-North Atlantic. *Geochemistry, Geophysics, Geosystems* 15:GC005453.
29. Tuite ML, Jr. & Macko SA (2013) Basinward nitrogen limitation demonstrates role of terrestrial nitrogen and redox control of δ15N in a Late Devonian black shale. *Geology* 41(10):1079-1082.
30. Lenton TM & Daines SJ (2017) Biogeochemical Transformations in the History of the Ocean. *Annual Review of Marine Science* 9(1):31-58.
31. Buick R (2007) Did the Proterozoic 'Canfield Ocean' cause a laughing gas greenhouse? *Geobiology* 5(2):97-100.
32. Freing A, Wallace DWR, & Bange HW (2012) Global oceanic production of nitrous oxide. *Philosophical transactions of the Royal Society of London. Series B, Biological sciences* 367(1593):1245-1255.
33. Heimhofer U*, et al.* (2018) Vegetation response to exceptional global warmth during Oceanic Anoxic Event 2. *Nature Communications* 9(1):3832.
34. Schmidtko S, Stramma L, & Visbeck M (2017) Decline in global oceanic oxygen content during the past five decades. *Nature* 542:335.
35. Bopp L*, et al.* (2013) Multiple stressors of ocean ecosystems in the 21st century: projections with CMIP5 models. *Biogeosciences* 10(10):6225-6245.
36. Bristow LA*, et al.* (2016) N_2 production rates limited by nitrite availability in the Bay of Bengal oxygen minimum zone. *Nature Geoscience* 10:24.
37. Naafs BDA*, et al.* (2016) Gradual and sustained carbon dioxide release during Aptian Oceanic Anoxic Event 1a. *Nature Geoscience* 9(2):135-139.
38. Turgeon SC & Creaser RA (2008) Cretaceous oceanic anoxic event 2 triggered by a massive magmatic episode. *Nature* 454(7202):323-326.
39. Lechler M, Pogge von Strandmann PAE, Jenkyns HC, Prosser G, & Parente M (2015) Lithium-isotope evidence for enhanced silicate weathering during OAE 1a (Early Aptian Selli event). *Earth and Planetary Science Letters* 432:210-222.
40. Hansell DA, Bates NR, & Olson DB (2004) Excess nitrate and nitrogen fixation in the North Atlantic Ocean. *Marine Chemistry* 84(3–4):243-265.

Figure Legends

Figure 1: Response of marine biogeochemistry to changes in ocean oxygenation

Response of biogeochemical processes to an increase in oceanic phosphate inventory for the Cenomanian simulations (pCO_2 at 1,120 ppmv). A) Ocean redox state with total oxygen content (O_2) of the ocean, extent of photic zone euxinia (PZE), extent of oceanic anoxia (0 µmol/l O_2), and rate of export production; B) Concentration of nitrate, ammonium, total fixed nitrogen (NO_3^- + NH_4^+), and phosphate concentration (in µmol N l^{-1}; multiplied by the Redfield N:P ratio); C)

Deviation of total fixed nitrogen to phosphate (N:P ratio) away from the 16:1 Redfield ratio, and D) Contribution of nitrogen fixation, ammonium assimilation, and nitrate assimilation to export production. Dashed lines represent values in modern-day simulation (1 x CO_2, 1 x PO_4^{3-} , and modern geography, ocean circulation and temperature). The 2 x PO_4^{3-} simulation is highlighted in red as this scenario has the best fit with proxy data for bottom water anoxia and photic zone euxinia (24).

Figure 2: Marine N-cycle during OAE 2 (4 x CO_2; 2 x PO_4^{3-})

A) Spatial distribution of the relative contribution to export production of N fixation (top), NH_4^+ assimilation (middle), and NO_3^- assimilation (bottom). Green ⊕ symbols reflect proxy records with a positive average $\delta^{15}N_{bulk}$ value across OAE 2, while pink ⊖ symbols reflect a negative average $\delta^{15}N_{bulk}$ value (see SI appendix for details); and B) Zonally averaged vertical concentration profiles of O_2 (top), NH_4^+ (middle), and NO_3^- (bottom). Both panels present model results using the OAE 2 analog simulation (Cenomanian paleography, 4 x CO_2; 2 x PO_4^{3-}).

Figure 3: Schematic of the marine nitrogen cycle's response to oceanic de-oxygenation

Schematic response of the marine N-cycle to a change in ocean oxygenation state, showing the transition from an oxic, nitrate-dominated ocean to an anoxic, ammonium-dominated ocean. Also shown is DIN_{xs} (DIN_{xs} = NO_3^- + NH_4^+ - 16 x PO_4^{3-}) (40). During OAE 2, the intermediate N-deficit state may have prevailed in which the ocean is anoxic enough to have lost most nitrate but has not yet developed very extensive OMZs rich in ammonium.

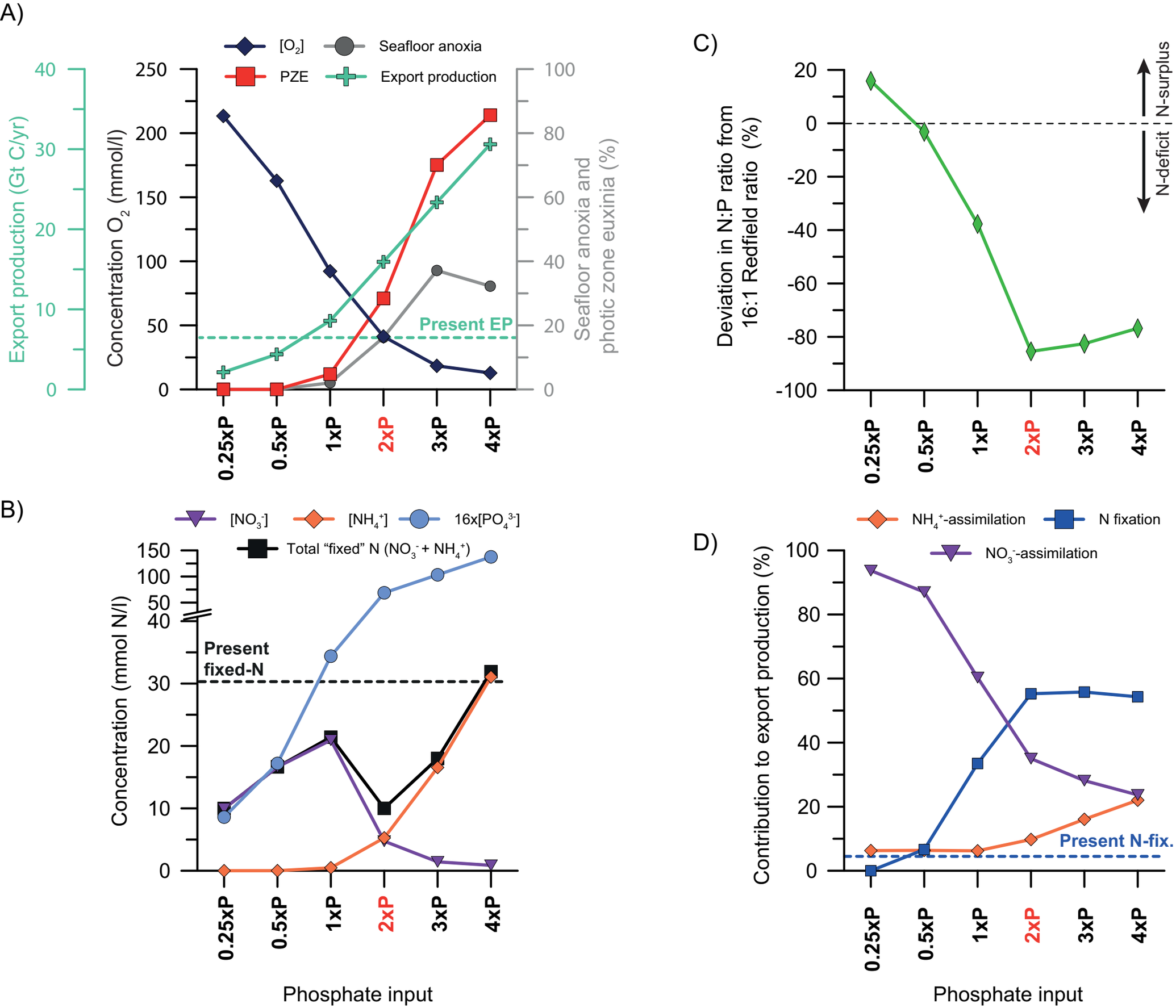
A)
[O2]
Seafloor anoxia
PZE
Export production
Export production (Gt C/yr)
Concentration O2 (mmol/l)
Seafloor anoxia and photic zone euxinia (%)
Present EP
0.25xP
0.5xP
1xP
2xP
3xP
4xP
B)
[NO3-]
[NH4+]
16x[PO43-]
Total "fixed" N (NO3- + NH4+)
Concentration (mmol N/l)
Present fixed-N
Phosphate input
C)
Deviation in N:P ratio from 16:1 Redfield ratio (%)
N-surplus
N-deficit
D)
NH4+-assimilation
N fixation
NO3-assimilation
Contribution to export production (%)
Present N-fix.
Phosphate input

A) Nitrogen contribution to export (%)

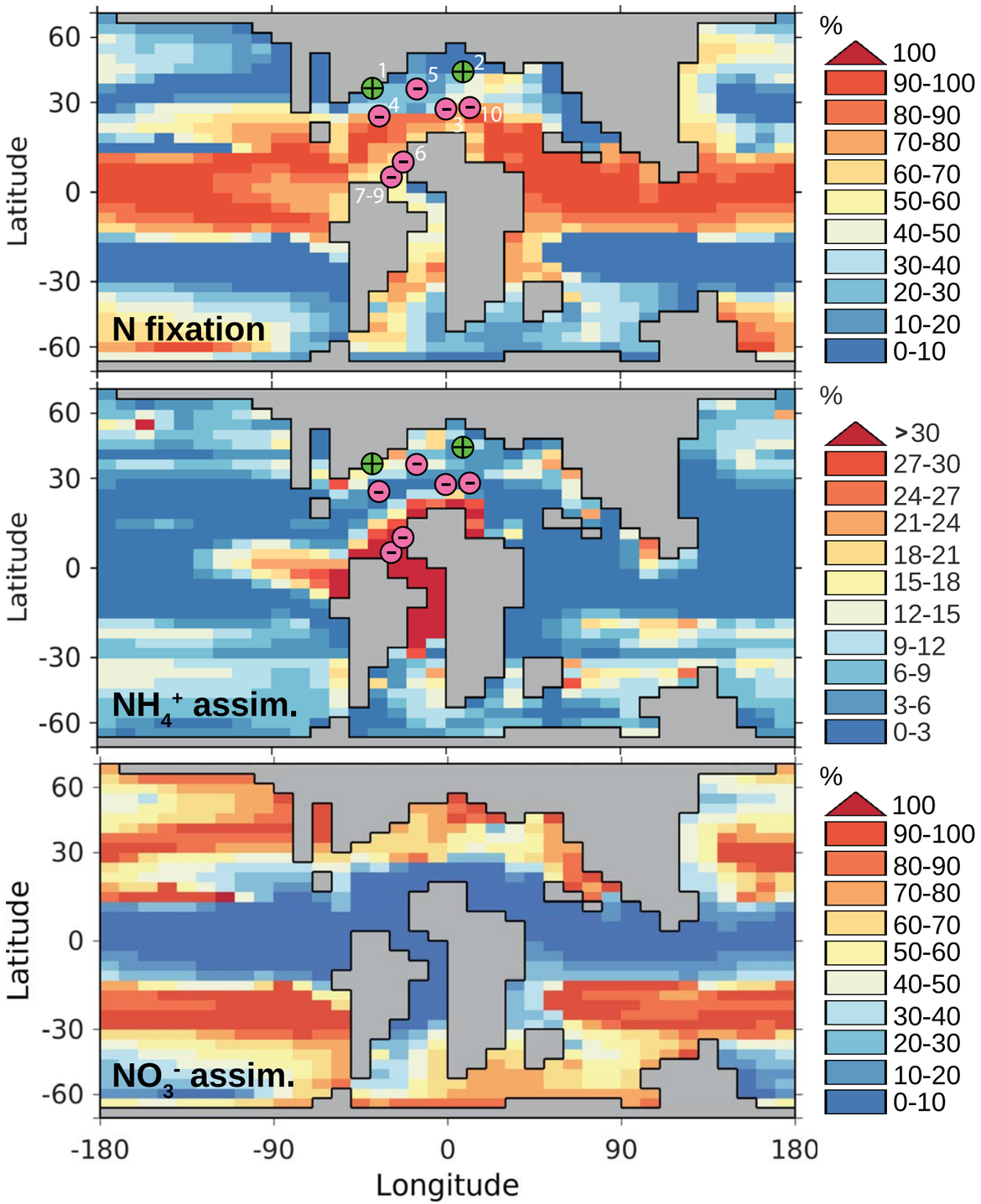

B) Zonally averaged vertical concentration profiles

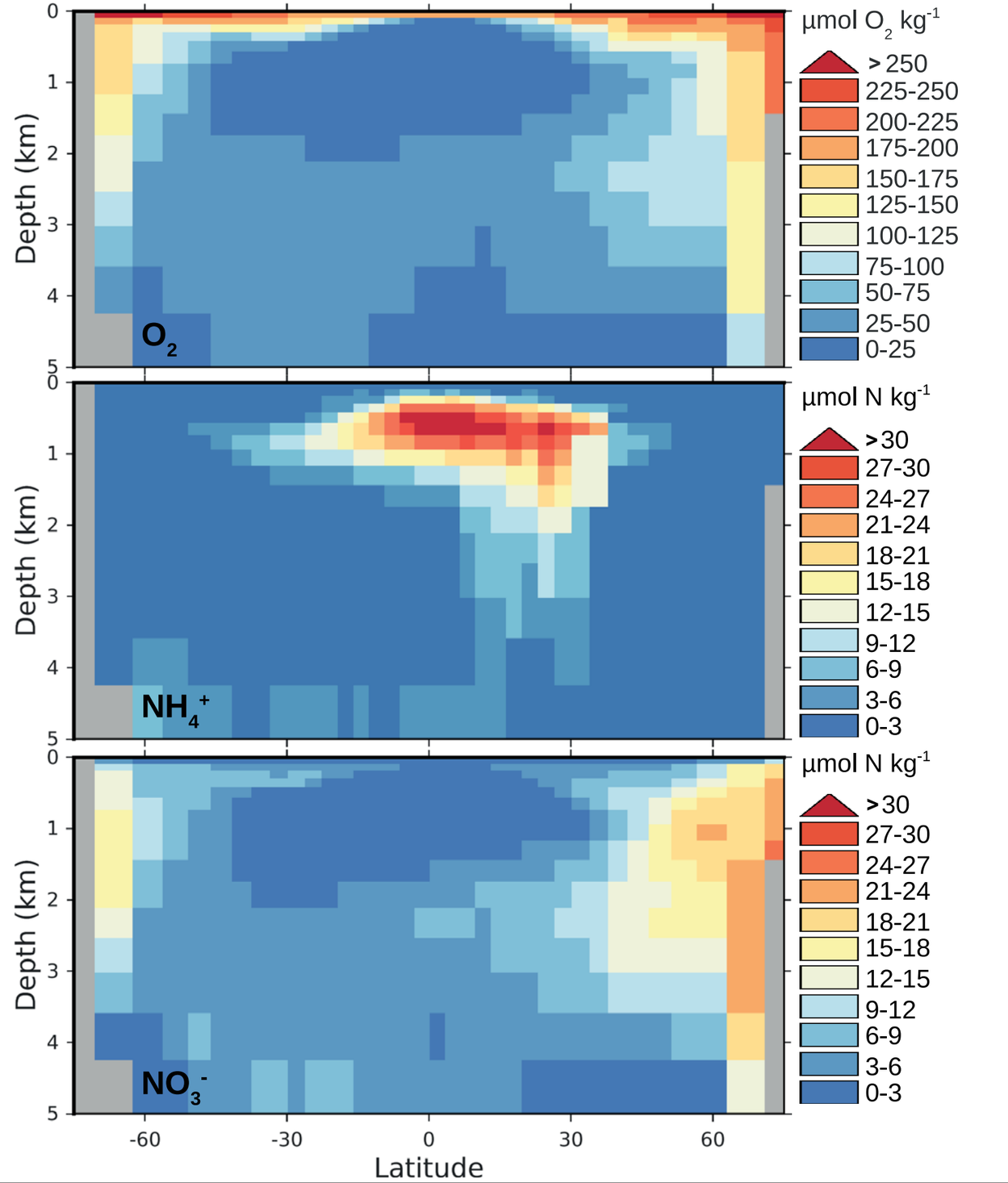

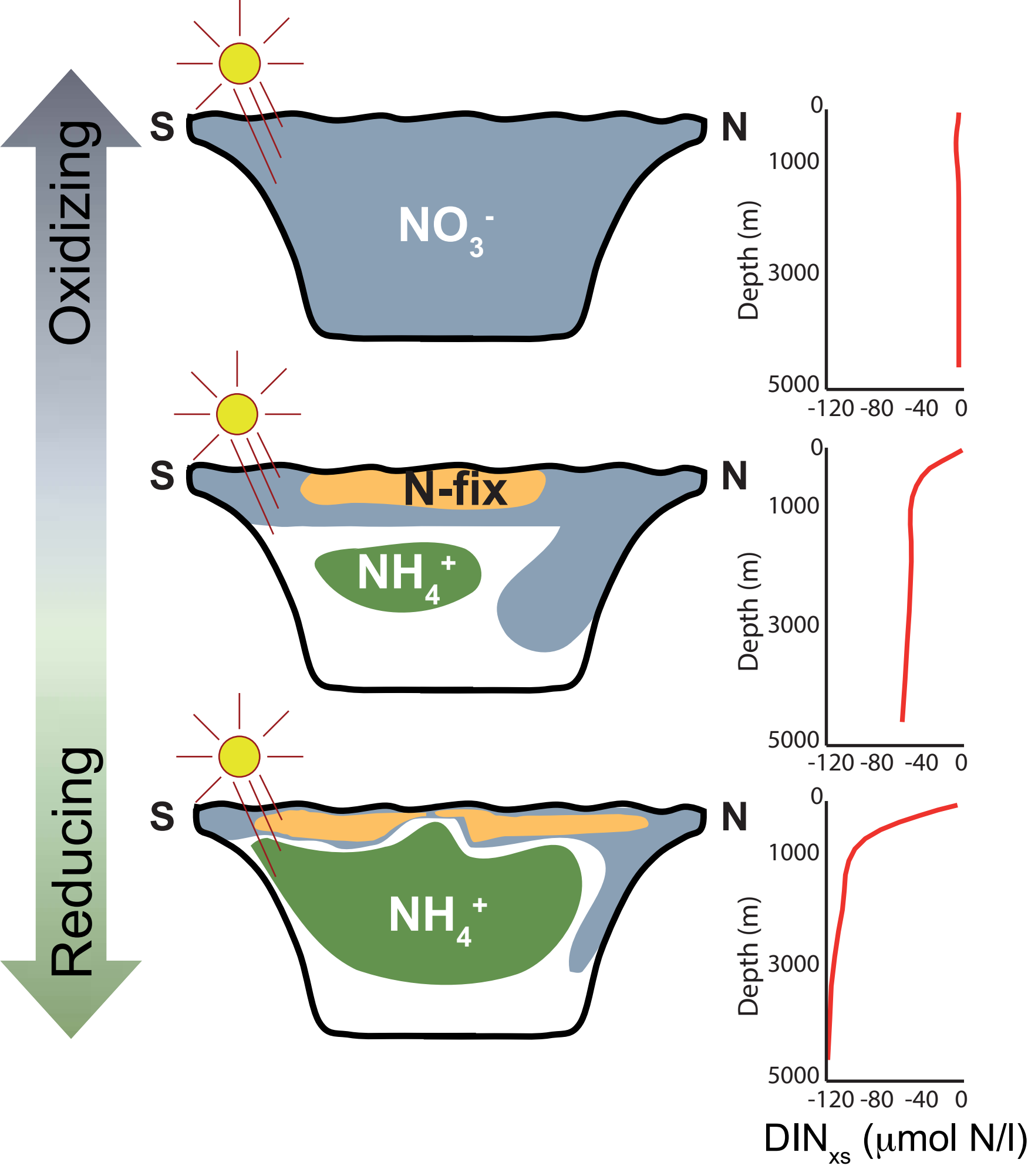
Oxidizing
Reducing
S
N
NO_3^-
N-fix
NH_4^+
NH_4^+
Depth (m)
0
1000
3000
5000
-120 -80 -40 0
DIN_{xs} (µmol N/l)